The effect of electron confinement on the transient velocity response in a superlattice miniband

1994 J. Phys.: Condens. Matter 6 3749

(http://iopscience.iop.org/0953-8984/6/20/013)

J. Phys.: Condens. Matter 6 (1994) 3749–3758. Printed in the UK

The effect of electron confinement on the transient velocity response in a superlattice miniband

X L Lei

China Centre of Advanced Science and Technology (World Laboratory), PO Box 8730, Beijing 100080, People's Republic of China and State Key Laboratory of Functional Material for Informatics, Shanghai Institute of Metallurgy, Chinese Academy of Sciences, 865 Changning Road, Shanghai, 200050, People's Republic of China

Received 22 November 1993

Abstract. The transient drift-velocity response of miniband transport to suddenly turned-on step electric fields is analysed for semiconductor superlattices with and without carrier transverse confinement. Our study is based on the recently developed balance-equation theory, which takes full account of the carrier occupation of the transverse subbands and the realistic electron–impurity and electron–phonon scatterings in the system. Up to 21 transverse subbands are included for two-dimensionally confined superlattices, and four lateral subbands for one-dimensionally confined ones. We find that thermal excitations of the carrier transverse movement suppress the Bloch oscillation. In a high-carrier-density system where carriers are thermalized rapidly in both longitudinal and transverse directions, the Bloch-type oscillatory velocity response, anticipated from purely one-dimensional Esaki–Tsu and Boltzmann theories, can appear only in extreme two-dimensionally confined system.

1. Introduction

The striking phenomenon of Bragg-diffraction-induced negative differential conductivity (NDC) in superlattice vertical transport, predicted by Esaki and Tsu [1] more than twenty years ago, has recently been demonstrated experimentally [2–4]. It is suggested that NDC can also be considered as a manifestation of the electric-field-induced progressive localization in superlattices [3, 5]. In view of enhanced scatterings resulting from carrier heating at high electric fields, however, a band model is still believed applicable for the electric field E of strength up to a substantial part of Δ/ed (Δ being the miniband width, d the superlattice period and e the electron charge), before the Stark quantized energy eEd reaches the miniband width. The role of electron heating, carrier statistics and realistic scattering mechanisms in superlattice miniband transport have been included in a balance-equation theory [6, 7], which nicely produces the experimental peak drift velocity v_p and the threshold electric field as functions of miniband width [6] and the low-temperature behaviour of v_p [8]. Parts of these effects have also been taken into account in the Boltzmann-equation approach to miniband conduction [9, 10]. These developments have definitely excluded previous doubts that NDC might be suppressed by the transverse degrees of freedom in the superlattice [11], stimulated further experimental and theoretical studies on the physics of miniband transport [12–15], and also brought about the prospect of superlattice-based transferred-electron microwave oscillators [16].

Although the existence of Wannier–Stark states and related Bloch oscillations has been demonstrated by optical measurements [17] in superlattices with dilute carriers, the possibility of an oscillatory current response of Bloch frequency to appear in the transient

0953-8984/94/203749+10$19.50

transport in high-carrier-density systems in which the steady-state conduction exhibits strong negative differential conductivity remains controversial. This issue not only has fundamental significance in understanding the physics, but also intimately relates to the formation time of the charged carrier-packet and thus affects the frequency attainable in transferred-electron microwave oscillators.

Theoretically, under the influence of a constant electric field a scattering-free electron in a superlattice miniband will oscillate at the Bloch frequency $\Omega_B = eEd/\hbar$. In a realistic many-electron system, in which impurity, phonon and intercarrier scatterings are unavoidable and electron heating (over all directions) and statistics also play important roles, the condition for a Bloch oscillation to survive is not clear. In the case of a three-dimensional superlattice, the preliminary calculation from the balance-equation theory found pronounced overshoot, but no Bloch-type oscillation showing up in the transient response to a suddenly turned-on electric field as high as 10 kV cm^{-1} [13]. On the other hand, calculation [9] based on the purely one-dimensional (1D) Boltzmann equation with constant scattering times indicated possible oscillatory velocity response to an electric-field suddenly switched on across the NDC region. Bloch-type oscillatory transient velocity can also be obtained using the balance-equation approach [18] for extremely two-dimensionally confined superlattices with realistic impurity and acoustic phonon scatterings when taking only the lowest subband into account (polar optic phonon scatterings are prohibited). A very recent calculation for coupled square quantum boxes from the three-dimensional Boltzmann equation [19] produced similar results: damped Bloch-oscillation-type transient response is possible when polar optic-phonon scatterings are suppressed. However, the specifics of the Bloch oscillation damping, especially the critical role of the lateral degrees of freedom of carriers, have not yet been clearly determined.

In this paper we will give a systematic investigation of transient response in superlattices with and without lateral confinement to step electric fields of differing strengths. Our approach is based on the recently developed balance-equation theory extended to the cases with 1D or 2D confinements [6, 7]. This theory is suitable for systems with high carrier density. In the calculation we consider as many subbands as required at the highest field discussed. Since realistic electron–impurity and electron–phonon scatterings are taken into full account in the balance-equation theory, transport properties can be evaluated from known scattering information of the material. It is thus possible to give a clear determination for the Bloch oscillation damping in the transient current response of superlattice miniband transport.

2. Time-dependent balance equations

We consider a model superlattice system in which electrons can move along the z-direction through the (lowest) miniband formed by the periodic potential wells and barriers of finite height. In the transverse (x–y) plane we consider three different cases: (1) electrons are confined to a small cylindrical region of diameter d_r by an infinitely high potential wall (1D superlattice or 2D-confined superlattice); (2) electrons move freely along the y-direction but are confined in a narrow well of width d_x in the x-direction by an infinitely high potential wall (2D superlattice or 1D-confined superlattice); (3) electrons move freely in both x and y directions (3D superlattice or unconfined superlattice).

The electron energy dispersion can be written as the sum of a transverse-motion energy $\epsilon_{n_\parallel}$ and a tight-binding-type miniband energy $\epsilon(k_z)$ related to the longitudinal motion:

$$\epsilon_{n_\parallel}(k_z) = \epsilon_{n_\parallel} + \epsilon(k_z) \tag{1}$$

with

$$\epsilon(k_z) = \frac{\Delta}{2}(1 - \cos k_z d) \tag{2}$$

where $-\pi/d < k_z \leqslant \pi/d$, d is the superlattice period along the z-direction, and Δ is the miniband width. The electron transverse state and its energy are described by the transverse quantum number $n_\parallel = (n_x, n_y)$. They should be specified separately for 1D, 2D and 3D superlattices.

The Lei–Ting balance-equation theory [20] has recently been extended to the system with an arbitrary energy band [6, 7], in which a transport state is described by the centre-of-mass (CM) momentum $P_d \equiv Np_d$ (N is the total number of carriers) and the relative electron temperature T_e. When a time-dependent but spatially uniform electric field $E(t)$ is applied along the z-direction, the balance equations for a semiconductor superlattice, which are obtained by calculating the rates of change of the average electron drift velocity and the average electron energy per carrier, take the form

$$\frac{dv_d}{dt} = eE/m_z^* + A_i + A_p \tag{3}$$

$$\frac{dh_e}{dt} = eEv_d - W. \tag{4}$$

Here

$$v_d = \frac{2}{N}\sum_{n_\parallel, k_z} \frac{d\epsilon(k_z)}{dk_z} f\left(\bar{\epsilon}_{n_\parallel}(k_z),\, T_e\right) \tag{5}$$

is the CM velocity, or the average drift velocity of the carrier in the z-direction,

$$\frac{1}{m_z^*} = \frac{2}{N}\sum_{n_\parallel, k_z} \frac{d^2\epsilon(k_z)}{dk_z^2} f\left(\bar{\epsilon}_{n_\parallel}(k_z),\, T_e\right) \tag{6}$$

is the averaged inverse effective mass of the CM, and

$$h_e = \frac{2}{N}\sum_{n_\parallel, k_z} \epsilon_{n_\parallel}(k_z) f\left(\bar{\epsilon}_{n_\parallel}(k_z),\, T_e\right) \tag{7}$$

is the average electron energy per carrier. In these equations

$$f(\epsilon,\, T_e) \equiv \left\{\exp\left[(\epsilon - \mu)/T_e\right] + 1\right\}^{-1} \tag{8}$$

stands for the Fermi distribution function at the electron temperature T_e, μ is the chemical potential determined by the condition that the total number of electrons equals N:

$$N = 2\sum_{n_\parallel, k_z} f\left(\bar{\epsilon}_{n_\parallel}(k_z),\, T_e\right) = 2\sum_{n_\parallel, k_z} f\left(\epsilon_{n_\parallel}(k_z),\, T_e\right) \tag{9}$$

and

$$\bar{\epsilon}_{n_\parallel}(k_z) \equiv \epsilon_{n_\parallel} + \epsilon(k_z - p_d) \tag{10}$$

can be regarded as the 'relative electron energy'. The expressions for the impurity- and phonon-induced frictional accelerations, A_i and A_p, and the energy-transfer rate from the electron system to the phonon system, W, have been given in [14], [21] and [6] respectively for 1D, 2D and 3D superlattices, together with the form factors due to longitudinal and transverse wavefunctions.

The energy dispersion form (1) enables us to write the average drift velocity and the inverse effective mass as

$$v_e = v_m \alpha(T_e) \sin(z_d) \tag{11}$$

$$\frac{1}{m^*} = \frac{1}{M^*} \alpha(T_e) \cos(z_d) \tag{12}$$

with $v_m = \Delta d/2$, $1/M^* = \Delta d^2/2$, and

$$\alpha(T_e) = \frac{2}{N} \sum_{n_\parallel, k_z} \cos(k_z d) f(\epsilon_{n_\parallel}(k_z), T_e). \tag{13}$$

$\alpha(T_e)$ is a function of T_e, but independent of the parameter $z_d \equiv p_d d$.

With the help of these expressions we can write the force- and energy-balance equations as

$$\frac{1}{v_m} \frac{dv_d}{dt} = eE(t) d\alpha(T_e) \cos(z_d) + \frac{2}{\Delta d}(A_i + A_p) \tag{14}$$

$$\frac{2}{\Delta} \frac{dh_e}{dt} = eE(t) d\alpha(T_e) \sin(z_d) - \frac{2W}{\Delta}. \tag{15}$$

In the case of time-dependent transport the CM momentum and the electron temperature are time-dependent variables. It is convenient to express dv_d/dt and dh_e/dt on the left-hand sides of (14) and (15) in terms of the time derivatives of z_d and T_e:

$$\frac{1}{v_m} \frac{dv_d}{dt} = \alpha(T_e) \cos(z_d) \frac{dz_d}{dT_e} + \left(\frac{d\alpha}{dT_e}\right) \sin(z_d) \frac{dT_e}{dt} \tag{16}$$

$$\frac{2}{\Delta} \frac{dh_e}{dt} = \alpha(T_e) \sin(z_d) \frac{dz_d}{dt} - \left[\left(\frac{d\alpha}{dT_e}\right) \cos(z_d) - \frac{2}{\Delta}\left(\frac{dh_\parallel}{dT_e}\right)\right] \frac{dT_e}{dt}. \tag{17}$$

Here we have made use of the relation

$$h_e = h_\parallel + \frac{\Delta}{2} - \frac{\Delta}{2} \alpha(T_e) \cos(z_d) \tag{18}$$

in which

$$h_\parallel = \frac{2}{N} \sum_{n_\parallel, k_z} \epsilon_{n_\parallel} f(\epsilon_{n_\parallel}(k_z), T_e) \tag{19}$$

is the average transverse energy of the electron.

3. One-dimensional superlattices

In the case of a 1D superlattice the transverse quantum numbers $n_\parallel = (l, m)$ ($l = 1, 2, \ldots$ and $m = 0, \pm 1, \pm 1, \ldots$), and the transverse energy is given by [14]

$$\epsilon_{n_\parallel} = 2(x_l^m)^2/(m^* d_r^2) \tag{20}$$

where m^* is the electron band effective mass of the background bulk material, and x_l^m represents the lth zero of the mth-order Bessel function, i.e. $J_m(x_l^m) = 0$.

If only the lowest transverse subband is taken into account, i.e. $dh_\parallel/dT_e$ in (17) is set to zero, balance equations (14) and (15) are reduced to the following simple form:

$$\frac{dz_d}{dt} = eE(t)d + \left[\frac{2(A_i + A_p)}{\Delta d} \cos(z_d) - \frac{2W}{\Delta} \sin(z_d)\right] \frac{1}{\alpha(T_e)} \tag{21}$$

$$\frac{dT_e}{dt} = \left[\frac{2(A_i + A_p)}{\Delta d} \sin(z_d) + \frac{2W}{\Delta} \cos(z_d)\right] \left(\frac{d\alpha}{dT_e}\right)^{-1}. \tag{22}$$

Based on this set of coupled differential equations for z_d and T_e, we have carried out a numerical calculation [18] at lattice temperature $T = 77$ K for a 1D GaAs-based superlattice having transverse diameter $d_r = 10$ mm, period $d = 15$ nm, miniband width $\Delta = 220$ K, and low-temperature (4.2 K) linear mobility $\mu_{(0)} = 1.0$ m^2 V s^{-1}. We assume a carrier sheet density of $N_s = 4.0 \times 10^{11}$ cm^{-2} (per period) in the transverse plane, corresponding to a line density $N_1 d = 0.314$. For this narrow miniband width the polar optic-phonon scattering is prohibited by the requirement of energy conservation. This greatly reduces the critical field E_c at which the steady-state drift velocity peaks. Both longitudinal and transverse acoustic phonons (through the deformation potential and piezoelectric couplings with electrons) are taken into account in the calculation. The calculated steady-state velocity-field relation and the transient velocity response to step electric fields turned on a time $t = 0$, having strengths $E = 60$ V cm^{-1} (a), $E = 130$ V cm^{-1} (b), $E = 250$ V cm^{-1} (c), $E = 0.5$ kV cm^{-1} (d), $E = 1$ kV cm^{-1} (e), $E = 2$ kV cm^{-1} (f), and $E = 4$ kV cm^{-1} (g), are plotted as dotted curves in figure 1. The steady-state critical field E_c is about 105 V cm^{-1} for this system. In the case of $E < E_c$ (a), there is no velocity overshoot in the transient response. Once the field strength $E > E_c$ (cases b, c and d) the velocity overshoot shows up, and becomes more pronounced at larger E. The oscillatory transient velocity begins to appear at a field strength about eight times the critical field E_c. At $E = 1$ kV cm^{-1} clear oscillations of the drift velocity are already seen, with an oscillatory period about 3.0 ps, a little larger than the free Bloch oscillation period $T_B = 2\pi/(eEd) = 2.76$ ps at this field. When the field strength further increases the transient velocity oscillation becomes increasingly stronger (f and g). For the cases of $E = 2$ kV cm^{-1} (f) and $E = 4$ kV cm^{-1} (g), the oscillation periods are 1.41 ps and 0.695 ps respectively, and the corresponding free Bloch periods are $T_B =$ 1.38 ps and 0.69 ps.

When higher transverse subbands are taken into consideration, both the steady-state $v_d - E$ relation and the transient response, though they remain the same at low electric fields, change remarkably at high electric fields. The solid curves shown in figure 1 are calculated results obtained from solving (14)–(17) by including 21 transverse subbands for the same system as described above. Since the electron temperature increases with increasing electric field, high-lying subbands are expected to affect transport behaviour greatly at high electric field even for this extremely 2D-confined system. We find that by taking many subbands into account the steady-state electron temperature T_e (not shown) at high field becomes much lower than that obtained in the one-subband-only case and the steady-state drift velocity becomes higher (figure 1(a)). The oscillatory response of the drift velocity weakens markedly: oscillatory behaviour begins to appear at higher electric field strength than the single-subband case and at the same field strength fewer oscillatory periods survive before approaching a final steady state (figure 1(e), (f)). The main difference between single-subband and multi-subband cases is that in the latter there is a non-zero average transverse energy $h_\parallel$ which increases with increasing electron temperature ($dh_\parallel/dT_e > 0$), indicating that the transverse movement of carriers in a superlattice suppresses the oscillation of its longitudinal transient velocity.

With increasing transverse diameter of the 1D superlattice, the energies of higher subbands are reduced quickly, and the role of the carrier transverse movement is expected to become more important. To see how the transient transport behaviour is affected by the transverse diameter d_r, we have calculated the transient drift velocity response at lattice temperature $T = 77$ K for a 1D-superlattice with transverse diameter $d_r = 20$ nm, period $d = 15$ nm, miniband width $\Delta = 220$ K, and low-temperature linear mobility $\mu(0) =$ 1.0 m^2 V^{-1} s^{-1}, to step electric fields (turned on at time $t = 0$) with strengths $E = 2$, 5, 10 and 20 kV cm^{-1} respectively. We still assume $N_s = 4.0 \times 10^{11}$ cm^{-2} (per period) for the

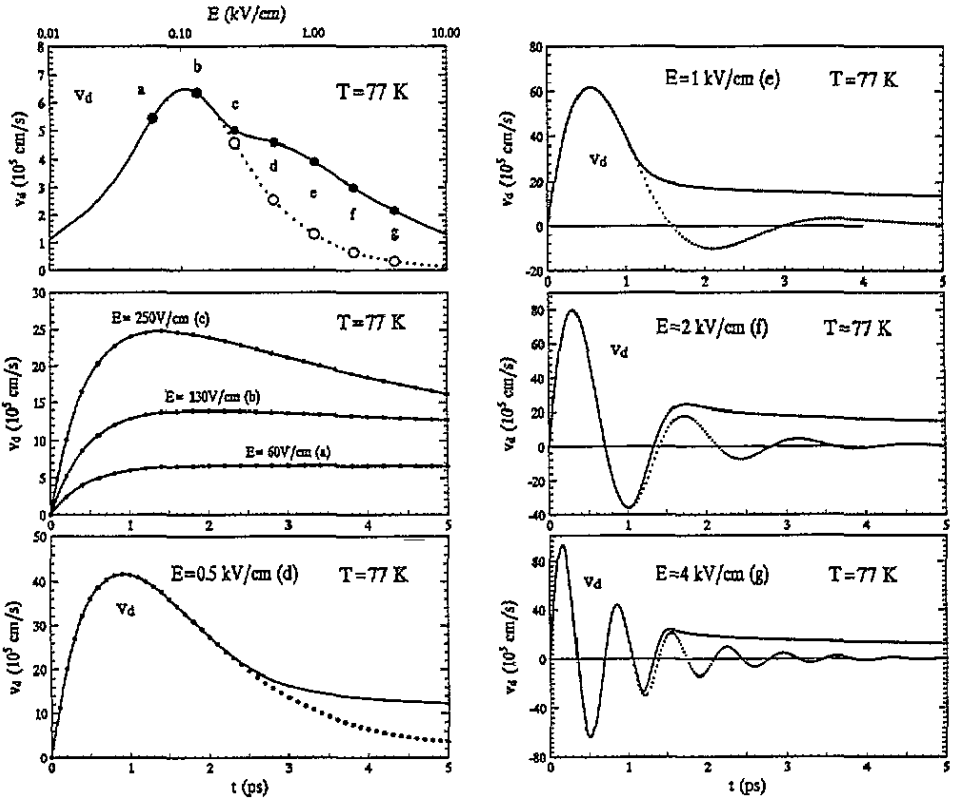

Figure 1. Steady-state drift velocity as a function of applied electric field (upper left corner), and the transient drift velocity response to step electric fields turned on at time $t = 0$ with different strengths (a)–(g) for a 1D superlattice of transverse diameter $d_r = 10$ nm, period $d = 15$ nm, miniband width $\Delta = 220$ K and carrier line density $N_1 d = 0.314$. Calculations are made at lattice temperature $T = 77$ K. The solid curves are results obtained by including 21 transverse subbands. For comparison the corresponding results obtained by considering only the lowest subband occupation are shown as dotted curves.

carrier sheet density in the transverse plane. This corresponds to a line density $N_1 d = 1.257$. 21 transverse subbands are included in the calculation. The calculated transient drift velocity v_d as a function of the time delay is shown in figure 2, together with the dc steady-state drift-velocity-field curve (inset). At this value of d_r the energy gaps between neighbouring transverse subbands are small enough to allow polar optical-phonon scattering to occur. This drastically changes both the steady-state and the transient transport behaviour. In the steady-state case the rise of the electron temperature with increasing electric field in the $d_r = 20$ nm system becomes much slower than that in the $d_r = 10$ nm system, and the peak drift velocity is reached at a much larger field strength ($E_c = 2.6$ kV cm^{-1}). The transient drift velocity response curve of the $d_r = 20$ nm system looks completely different from that of the $d_r = 10$ nm system: drift velocity exhibits only overshoot, without oscillation.

In figure 3 we show the transient drift velocity response to step electric fields of strengths $E = 1$, 2, 5 and 10 kV cm^{-1}, and the dc steady-state drift-velocity-field curve for a 1D-superlattice having transverse diameter $d_r = 40$ nm, period $d = 15$ nm, miniband width $\Delta = 220$ K, low-temperature linear mobility $\mu(0) = 1.0$ m^2 V^{-1} s^{-1} and carrier sheet density $N_s = 4.0 \times 10^{11}$ cm^{-2} (per period) in the transverse plane (equivalent to a line density

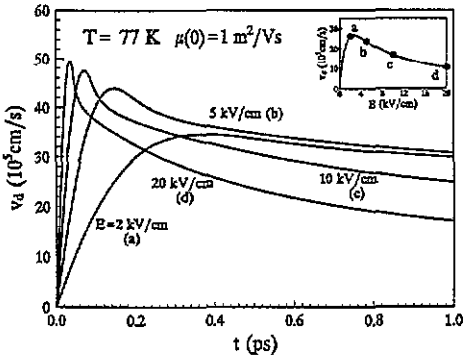

Figure 2. Transient drift velocity (v_d) response of a 1D superlattice with transverse diameter d_r = 20 nm, period d = 15 nm, miniband width Δ = 220 K, carrier line density, $N_1 d$ = 1.257 and low-temperature linear mobility $\mu(0)$ = 1.0 m^2 V^{-1} s^{-1}, to step electric fields turned on at time t = 0 with various field strengths. The inset shows the corresponding locations of these fields on the steady-state velocity-field curve. The lattice temperature is T = 77 K.

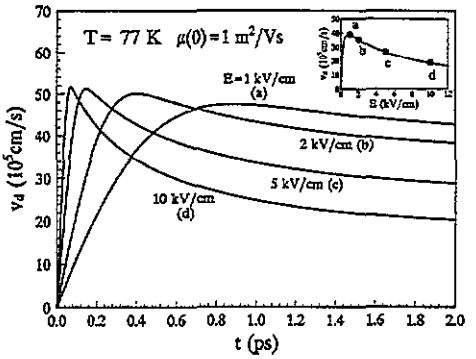

Figure 3. Transient drift velocity (v_d) response of a 1D superlattice, with transverse diameter d_r = 40 nm, period d = 15 nm, miniband width Δ = 220 K, carrier line density $N_1 d$ = 5.027 and low-temperature linear mobility $\mu(0)$ = 1.0 m^2 V^{-1} s^{-1}, to step electric fields turned on at time t = 0 with various field strengths. The inset shows the corresponding locations of these fields on the steady-state velocity-field curve. The lattice temperature is T = 77 K.

$N_1 d$ = 5.027). 21 transverse subbands are included in the calculation. For this value of d_r neighbouring subbands overlap with each other, and the steady-state transport behaviour is close to a corresponding unconfined superlattice. The transient drift velocity exhibits only overshoot, without oscillatory behaviour up to field strength E = 20 kV cm^{-1} (the curve for E = 20 kV cm^{-1} is similar but not shown in the figure).

4. Two-dimensional and three-dimensional superlattices

In the case of a 2D superlattice, the transverse quantum number $n_\parallel$ consists of a subband index n in the (confined) x-direction and a wavevector k_y in the y-direction: $n_\parallel = (n, k_y)$, n = 1, 2, ... The transverse energy is given by [21]

$$\epsilon_{n_\parallel} \equiv \epsilon_{n,k_y} = \frac{\pi^2(n^2-1)}{2m^* d_x^2} + \frac{k_y^2}{2m^*}. \tag{23}$$

Since electrons move freely along the y-direction in this system, the transverse movement is expected to play an even more important role in determining the transient behaviour of vertical transport.

To see this we have numerically calculated the transient drift velocity response shown in figure 4, at lattice temperature T = 45 K for a 2D superlattice having x-extension d_x = 45 nm, superlattice period d = 10 nm, miniband width Δ = 900 K, carrier 2D density N_2 = 9.0 × 10^{11} cm^{-2}, and low-temperature linear mobility $\mu(0)$ = 100 m^2 V^{-1} s^{-1}, to step electric fields turned on at time t = 0 having strengths E = 2, 5, 10 and 20 kV cm^{-1}. The steady-state $v_d - E$ curve is also plotted in the figure (inset). These four values of the field strengths (E = 2, 5, 10 and 20 kV cm^{-1}) are in the negative differential mobility region. Four transverse subbands together with the intrasubband and intersubband impurity and phonon scatterings are included in both the steady and transient calculations. Although such a low lattice temperature and high impurity-limited mobility should offer a minimum frictional-force environment for a Bloch-type oscillatory transient response to occur, the

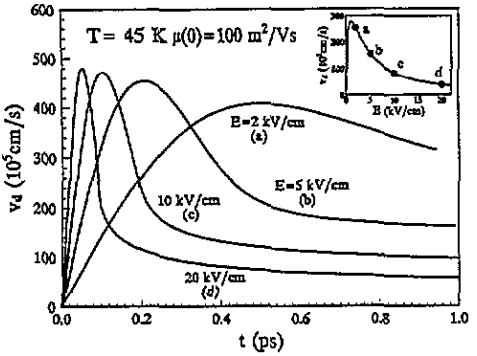

Figure 4. Transient drift velocity (v_d) response of a 2D superlattice, with x-extension d_x = 45 nm, period d = 10 nm, miniband width Δ = 900 K, carrier 2D density N_2 = 9.0 × 10^{11} cm^{-2} and low-temperature linear mobility $\mu(0)$ = 100 m^2 V^{-1} s^{-1}, to step electric fields turned on at time t = 0 with various strengths. The inset shows the corresponding locations of these fields on the steady-state velocity-field curve. The lattice temperature is T = 45 K.

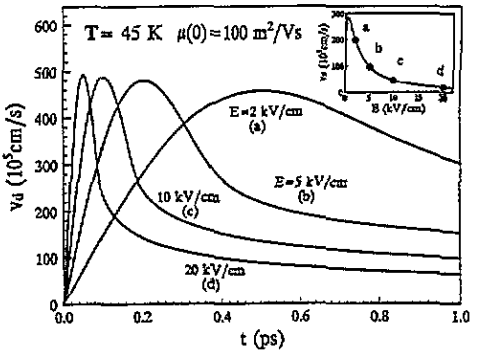

Figure 5. Transient drift velocity (v_d) response of a 3D superlattice, with period d = 10 nm, miniband width Δ = 900 K, carrier sheet density N_s = 2.0 × 10^{11} cm^{-2} and low-temperature linear mobility $\mu(0)$ = 100 m^2 V^{-1} s^{-1}, to step electric fields turned on at time t = 0 with various strengths. The inset shows the corresponding locations of these fields on the steady-state velocity-field curve. The lattice temperature is T = 45 K.

numerical results obtained from balance equations (14)–(17) exhibit only pronounced drift velocity overshoot, without any trace of Bloch-type oscillatory behaviour for electric fields as high as E = 20 kV cm^{-1}, as shown in figure 4.

In fact, the transient behaviour of the drift velocity response in such a 2D superlattice is already quite similar to that of an unconfined superlattice (3D superlattice). In figure 5 we show the calculated transient drift velocity response at lattice temperature T = 45 K for a 3D superlattice, having period d = 10 nm, miniband width Δ = 900 K, low-temperature linear mobility $\mu(0)$ = 100 m^2 V^{-1} s^{-1} and carrier sheet density N_s = 2.0 × 10^{11} cm^{-2}, to step electric fields turned on at time t = 0 having strengths E = 2, 5, 10 and 20 kV cm^{-1}. This value of carrier sheet density N_s implies an average carrier bulk density of $n = N_s/d$ = 2.0 × 10^{19} cm^{-3}, equal to the average carrier bulk density of the 2D superlattice described in figure 4: $n = N_2/d_x$. The steady-state $v_d - E$ behaviour of this system is also shown in the inset. The transient drift velocities of these two systems are indeed quite similar.

Impurity scattering greatly affects both the steady-state and the transient transport behaviour. We show in figure 6 the steady-state $v_d - E$ curve and the transient drift velocity response at lattice temperature T = 45 K, for a 3D superlattice with period d = 10 nm, miniband width Δ = 900 K and carrier sheet density N_s = 2.0 × 10^{11} cm^{-2}, exactly the same as the system described in figure 5, but having a stronger impurity scattering: low-temperature linear mobility $\mu(0)$ = 1.0 m^2 V^{-1} s^{-1}. Stronger impurity scattering reduces the rising speed of the drift velocity at the initial stage of the transient transport and thus suppresses the maximum drift velocity, which is reached at a time delay slightly less than a quarter of the Bloch period $T_B = 2\pi/(eEd)$.

Finally, in order to show the effect of the lattice temperature on the transient transport we plot in figure 7 the steady-state $v_d - E$ curve and the transient drift velocity response at lattice temperature T = 300 K, for a 3D superlattice similar to that described in figure 6: period d = 10 nm, miniband width Δ = 900 K, carrier sheet density N_s = 1.5 × 10^{11} cm^{-2} and low-temperature linear mobility $\mu(0)$ = 1.0 m^2 V^{-1} s^{-1}. The transient response behaviour of the drift velocity is similar to that of the T = 45 K case, but maximum velocities attainable are reduced in comparison with figure 6.

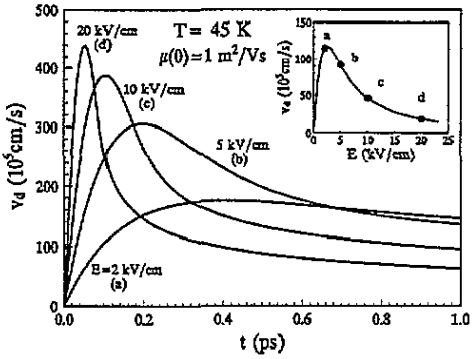

Figure 6. Transient drift velocity (v_d) response of a 3D superlattice, with period d = 10 nm, miniband width Δ = 900 K, carrier sheet density $N_s = 2.0 \times 10^{11}$ cm^{-2} and low-temperature linear mobility $\mu(0) = 1.0$ m^2 V^{-1} s^{-1}, to step electric fields turned on at time $t = 0$ with various strengths. The inset shows the corresponding locations of these fields on the steady-state velocity-field curve. The lattice temperature is T = 45 K.

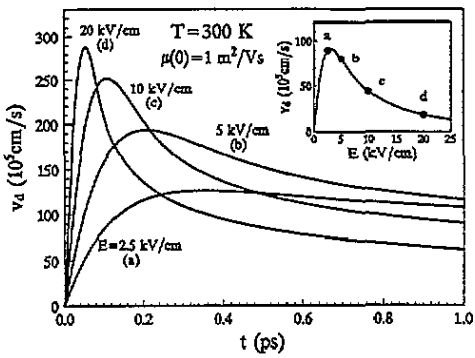

Figure 7. Transient drift velocity (v_d) response of a 3D superlattice, with period d = 10 nm, miniband width Δ = 900 K, carrier sheet density $N_s = 1.5 \times 10^{11}$ cm^{-2} and low-temperature linear mobility $\mu(0) = 1.0$ m^2 V^{-1} s^{-1}, to step electric fields turned on time $t = 0$ with various strengths. The inset shows the corresponding locations of these fields on the steady-state velocity-field curve. The lattice temperature is T = 300 K.

5. Conclusions

We have systematically investigated the transient drift velocity response of miniband transport in superlattices with and without carrier transverse confinement to step electric fields of different strengths. Our study is based on the recently developed balance-equation theory for miniband transport which takes account of the carrier transverse movement and the realistic electron–impurity and the electron–phonon scatterings in the system. This theory, which employs a unique electron temperature to describe the carrier occupation of both the longitudinal and the transverse states of the many-electron system, thus assuming the rapid thermalization of the carriers in all directions, should be valid for higher carrier density cases, as discussed in this paper. We find that the Bloch-type oscillatory transient velocity can appear only in extreme laterally (2D-) confined systems. Thermal excitations of the carrier transverse movement suppress the Bloch oscillation of the drift velocity. In a system where carriers are thermalized rapidly in all directions, direct observation of the Bloch-type oscillatory current in the transient miniband transport of a GaAs-based 1D superlattice (2D-confined superlattice) with lateral confinement of the order of 20 nm or larger is improbable. The transient miniband response of a 2D superlattice (1D-confined superlattice) behaves like an unconfined one: the drift velocity may exhibit a very pronounced overshoot, but no Bloch-type oscillation. This is at variance with what is anticipated from purely 1D Boltzmann-type theories, which essentially describe dilute carriers in a superlattice miniband.

Acknowledgment

The author wishes to thank the National Natural Science Foundation of China for support of this work.

References

[1] Esaki L and Tsu R 1970 *IBM J. Res. Dev.* **14** 61
[2] Sibille A, Palmier J F, Wang H and Mollot F 1990 *Phys. Rev. Lett.* **64** 52
[3] Beltram F, Capasso F, Sivco D L, Hutchinson A L and Chu S N G 1990 *Phys. Rev. Lett.* **64** 3167
[4] Grahn H T, von Klitzing K, Ploog K and Döhler G H 1991 *Phys. Rev.* B **43** 12094
[5] Tsu R and Esaki L 1991 *Phys. Rev.* B **43** 5204
[6] Lei X L, Horing N H M and Cui H L 1991 *Phys. Rev. Lett.* **66** 3277
[7] Lei X L 1992 *Phys. Status Solidi* b **170** 519
[8] Lei X L 1992 *J. Phys.: Condens. Matter* **4** L659
[9] Ignatov A A, Dodin E P and Shaskin V I 1991 *Mod. Phys. Lett.* B **5** 1087
[10] Sibille A 1993 *Superlatt. Microstruct.* **13** 247
[11] Kroemer H 1977 *Phys. Rev.* B **15** 880
[12] Lei X L and da Cunha Lima I C 1992 *J. Appl. Phys.* **71** 5517
[13] Lei X L, Horing N J M and Cui H L 1992 *Mod. Phys. Lett.* B **6** 1075; 1992 *J. Phys.: Condens. Matter* **4** 9375
[14] Lei X L 1992 *J. Phys.: Condens. Matter* **4** 9367
Lei X L and Wang X F 1993 *J. Appl. Phys.* **73** 3867
[15] Gerhardts R R 1993 *Phys. Rev.* B **48** 9178
[16] Hadjazi M, Sibille A, Palmier P J and Mollot F 1992 *Electron. Lett.* **27** 1101
[17] Feldmann J, Leo K, Shah J, Miller D A B, Cunningham J E, Meier T, von Plessen G, Schulze A, Thomas P and Schmitt-Rink S 1992 *Phys. Rev.* B **46** 7252
Leo K, Bolivar P H, Brüggemann F, Schwedler R and Köhler K 1992 *Solid State Commun.* **84** 943
[18] Lei X L 1993 *J. Phys.: Condens. Matter* **5** L43
[19] Noguchi H, Leburton J P and Sakaki H 1993 *Phys. Rev.* B **47** 15593
[20] Lei X L and Ting C S 1984 *Phys. Rev.* B **30** 4809; 1985 *Phys. Rev.* B **32** 1112
[21] Lei X L, Horing N J M, Cui H L and Thornber K K 1993 *Phys. Rev.* B **48** 5366; 1993 *Solid State Commun.* **86** 231